

# Supporting Information

Hussain et al. 10.1073/pnas.1014299107

## SI Text

**Heteronuclear Single Quantum Coherence Titrations.** NMR experiments were performed on a Bruker 600 MHz NMR spectrometer equipped with triple resonance cryoprobe. Uniform nitrogen labeling in Pab-NTD was achieved by its expression in minimal media containing  $^{15}\text{NH}_4\text{Cl}$  as the sole nitrogen source. In order to check the binding of Ser3AA and Thr3AA, U- $^{15}\text{N}$  Pab-NTD [200  $\mu\text{M}$  in 50 mM phosphate buffer (pH 7.2) containing 50 mM NaCl,  $T = 298\text{ K}$ ] was titrated with substrate analogs. Chemical shift perturbations in Pab-NTD upon titration were monitored by a series of two-dimensional  $^{15}\text{N}$ - $^1\text{H}$  HSQC spectra ( $1,024 \times 256$  points) collected with increasing concentrations of ligand. Three datasets were recorded for effective ligand concentration of 0  $\mu\text{M}$ , 100  $\mu\text{M}$ , and 500  $\mu\text{M}$  of Ser3AA and Thr3AA.

**Isothermal Titration Calorimetry.** The in vitro binding of substrate analogs to Pab-NTD was measured by isothermal titration calorimetry (ITC) using a VP-ITC calorimeter (MicroCal). ITC Buffer (20 mM Tris, pH 7.5) was used for diluting the protein and dissolving substrate analogs. All samples were degassed prior to titration. The 50  $\mu\text{M}$  protein sample (1.4 mL) was titrated against 300  $\mu\text{L}$  of 0.8 mM substrate over 30 injections at 303 K. For Thr3AA titration, 100  $\mu\text{M}$  protein sample (1.4 mL) was titrated against 300  $\mu\text{L}$  of 2.0 mM substrate over 20 injections at 303 K. Similarly, the heat of dilution of analogs was measured by a blank titration of ligands into the buffer, and this was subtracted from the binding isotherms of Pab-NTD. The change in heat of the proteins upon titrating with analogs was measured, integrated, and fitted into a one-site binding model for calculation of association constant ( $K_a$ ),  $\Delta H_{\text{app}}$ , and  $T\Delta S$  using the Origin 7.0 software (MicroCal) for curve fitting and data analysis. The parameters  $K_d$  and  $\Delta G$  were calculated using formulae  $K_d = 1/K_a$  and  $\Delta G = \Delta H - T\Delta S$ , respectively.

**Crystallization, Structure Determination, and Refinement.** The nonhydrolyzable analog Thr3AA was bought from Jena Biosciences, and

Ser3AA, Gly3AA, and ThrAMS from RNA-Tech. The analogs were dissolved in 20 mM Tris (pH 9.0) (ThrAMS in pH 7.5), and used for crystallization at varying concentrations. Pab-NTD was purified and the complexes were crystallized in similar conditions as mentioned earlier (1). Data were collected at 100 K on an in-house MAR research MAR-345dtb image plate detector with X-rays generated by a Rigaku RU-H3R rotating anode generator equipped with an Osmic mirror system, operated at 50 kV and 100 mA. The X-ray diffraction datasets were processed using DENZO and subsequent scaling and merging of intensities were carried out using SCALEPACK (2). The complex structures were solved using MOLREP-AUTO MR as implemented in CCP4 suite (3) by using Pab-NTD structure (4) as the model (PDB id: 1Y2Q). The Lys121 in the Pab-NTD wild type coordinates were mutated to Ala in order to get an unbiased electron density of Lys121 side chain in the case of Ser3AA and Thr3AA complexes.

CNS (5) was used for refinement and iterative rounds of model building and water picking was done in "O" (6). The parameters for refinement of ligands were obtained from PRODRG server (7). The model was finally verified by PROCHECK (8) and figures were prepared by SETOR (9) and PYMOL (10).

It is worth adding here that attempts to capture free Thr in Pab-NTD even at higher concentrations (1 : 50) were unsuccessful as no electron density corresponding to Thr was observed (Table S2). However, the absence of free Thr from the editing pocket of Pab-NTD is not surprising as it is neither the substrate nor the product of its enzymatic action. Attempts to capture Ser2AA and Gly2AA, mimicking Ser and Gly attached to 2' OH of tRNA, at higher concentrations (1 : 50) in the given crystallization conditions were unsuccessful as no electron density corresponding to the analogs was observed (Table S2). The absence of electron density for Ser2AA and Gly2AA analogs is in accordance with our earlier proposed hypothesis that Pab-NTD specifically binds amino acid attached at 3' OH position of terminal ribose of tRNA<sup>Thr</sup> (1).

1. Hussain T, et al. (2006) Posttransfer editing mechanism of a D-aminoacyl-tRNA deacylase-like domain in threonyl-tRNA synthetase from archaea. *EMBO J.* 25:4152–4162.
2. Otwinowski Z, Minor W, (1997) Processing of X-ray diffraction data collected in oscillation mode. *Methods Enzymol.* 276:307–326.
3. CCP4 (1994) The CCP4 suite: programs for protein crystallography. *Acta Crystallogr. D* 50:760–764.
4. Dwivedi S, Kruparani, SP, Sankaranarayanan R (2005) A D-amino acid editing module coupled to the translational apparatus in archaea. *Nature Struct. Mol. Biol.* 12:556–557.
5. Brünger AT, et al. (1998) Crystallography and NMR system: a new software suite for macromolecular structure determination. *Acta Crystallogr. D* 54:905–921.
6. Jones TA, Zou JY, Cowan SW, Kjeldgaard M (1991) Improved methods for building protein models in electron density maps and the location of errors in these models. *Acta Crystallogr. A* 47:110–119.
7. Schuettelkopf AW, van Aalten DMF (2004) PRODRG—a tool for high-throughput crystallography of protein-ligand complexes. *Acta Crystallogr. D* 60:1355–1363.
8. Laskowski RA, MacArthur MW, Moss DS, Thornton JM (1993) PROCHECK: a program to check the stereochemical quality of protein structures. *J. Appl. Cryst.* 26:283–291.
9. Evans SV, (1993) SETOR: hardware lighted three-dimensional solid model representations of macromolecules. *J. Mol. Graphics* 11:134–138.
10. DeLano WL (2002) PyMol <http://www.pymol.org>

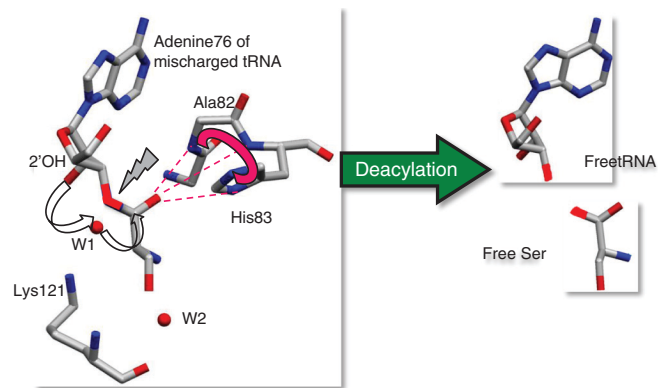


**Fig. S1.** Substrate-assisted catalysis of mischarged Ser-tRNA<sup>Thr</sup> in Pab-NTD [as proposed in earlier study (1)]. The mutation of Lys121 to Met, the only side chain in the vicinity that helps in the positioning of W1, shows deacylation activity and suggests that the Lys121 does not play a catalytic role. We have earlier mutated several residues in the vicinity of the scissile bond and showed that none of them completely abolished the deacylation activity (1). Therefore, in the absence of any side chain involvement, the 2' OH of the ribose is the only candidate that can act as a general base and play the critical role of activating W1 to have a nucleophilic attack on the carbonyl carbon of the Ser-tRNA<sup>Thr</sup> in a substrate-assisted catalysis manner. The tetrahedral intermediate formed can be stabilized in Pab-NTD by the oxyanion hole formed by the main chain nitrogen atom of Ala82 and main chain as well as side chain nitrogen atoms of His83.

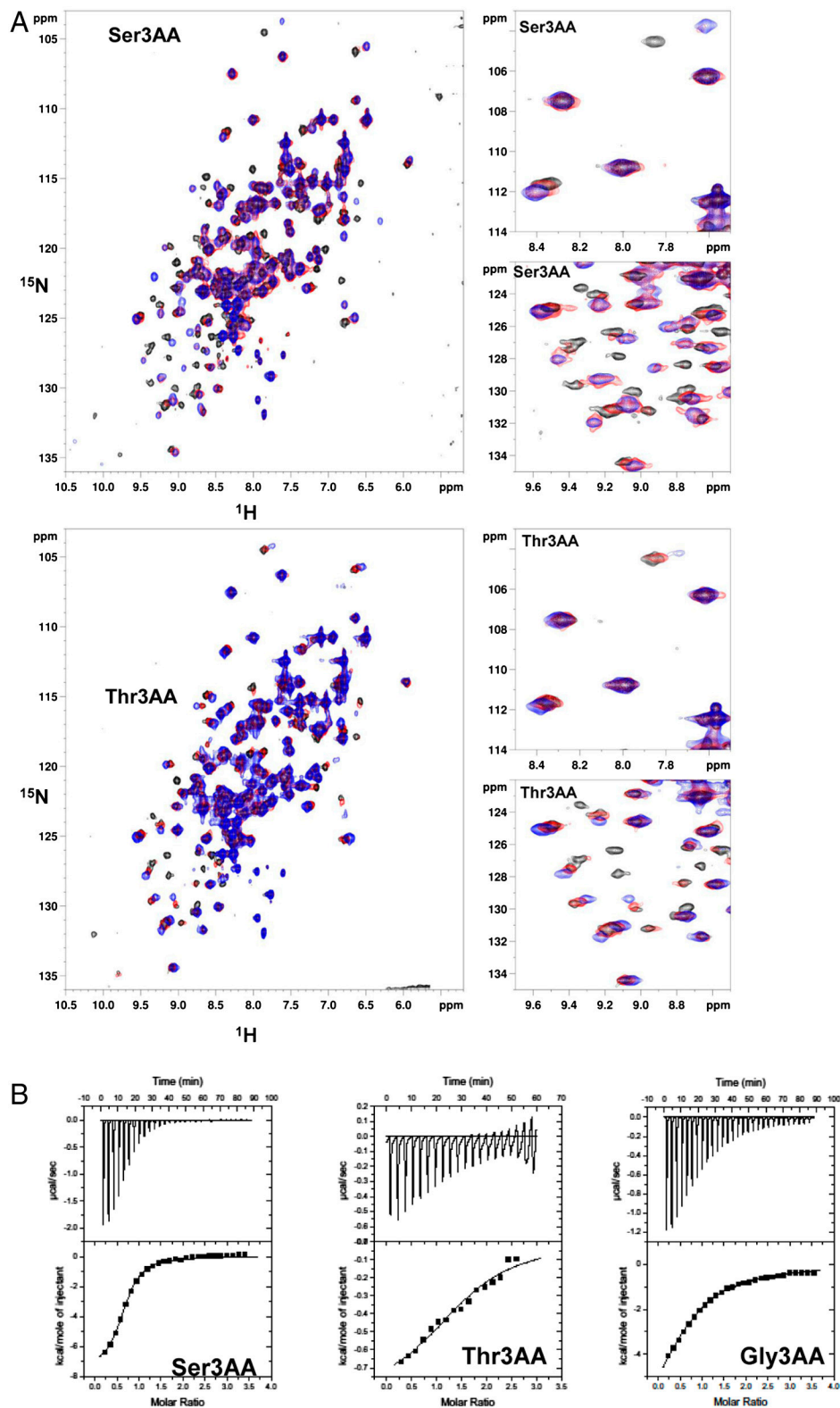


**Fig. S2.** Binding studies of substrate analogs. (A) Overlay of  $^{15}\text{N}$ - $^1\text{H}$  HSQC titrations on U- $^{15}\text{N}$  labeled Pab-NTD (200 mM) with increasing concentrations (0 mM: Black, 100 mM: Red, and 500 mM: Blue) of Ser3AA (top) and Thr3AA (below). Right shows two representative excerpts for a closer view. (B) Binding isotherm of Pab-NTD titrated against substrate analogs. Top: Raw titration curve; Bottom: Nonlinear regression curve fitting of heats by using one-site binding model. The thermodynamic parameters of binding are mentioned in Table 1.

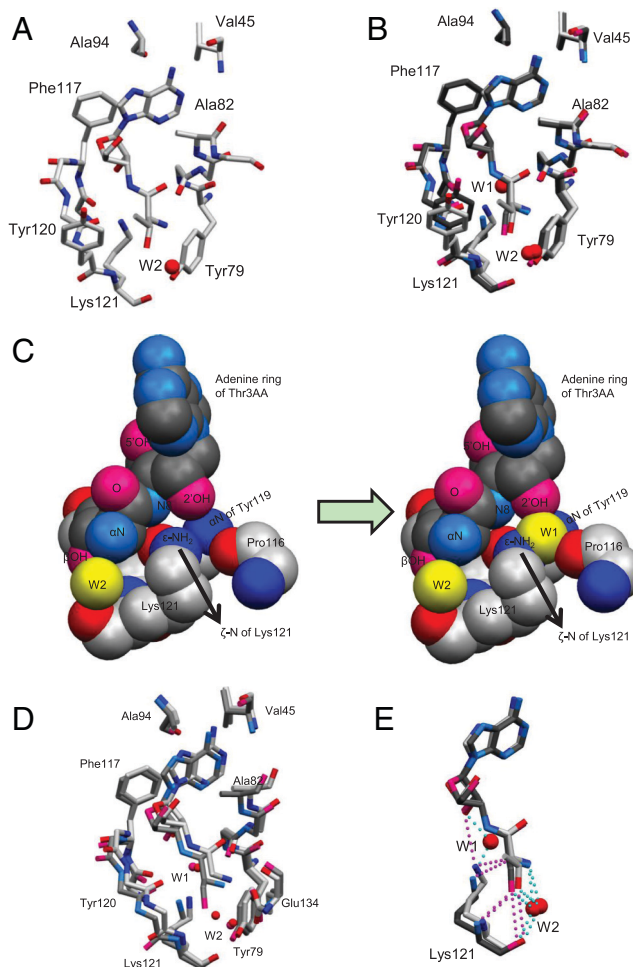


**Fig. S3.** Posttransfer substrate analog complexes with Pab-NTD. (*A*): Close view of Thr3AA and residues in the editing pocket of Pab-NTD in Pab-NTD-Thr3AA complex. (*B*): Superposition of the Pab-NTD-Ser3AA complex (darker shade) on Pab-NTD-Thr3AA complex (lighter shade) shows similar positioning of Ser3AA and Thr3AA as well as of residues in the editing pocket. Repositioning of Tyr120 and Lys121 can be seen. (*C*): Thr3AA shown in darker shade in editing pocket of Pab-NTD (shown in lighter shade). Only Lys121 and main chain atoms of Pro116 and Tyr119 are shown. The van der Waals radius of each atom is depicted. There is no space for catalytic water due to repositioning of Lys121 side chain in Pab-NTD-Thr3AA complex. Modeling of W1 in Pab-NTD-Thr3AA complex shows steric hindrance to Lys121, Pro116, and 2' OH of Thr3AA as shown in the right hand side figure. (*D*): Superposition of Pab-NTD-Ser3AA (darker shade) and Pab-NTD-Gly3AA (lighter shade) complexes. The absence of side chain in Gly3AA leads to a significant change (0.8–1.74 Å) in  $C_{\alpha}$  position when compared with that of Ser3AA. The anchoring of the side chain by hydrogen bonding plays an important role in fixing the substrate in the editing pocket. (*E*): Lys121 utilizes all its anchoring points to make direct or water-mediated interaction with Ser3AA (darker shade) and Thr3AA (lighter shade) in the editing pocket. Lys121 side chain in Pab-NTD-Thr3AA complex sterically excludes W1. Subtle change in the  $C_{\beta}$  position of Ser3AA and Thr3AA can also be seen.

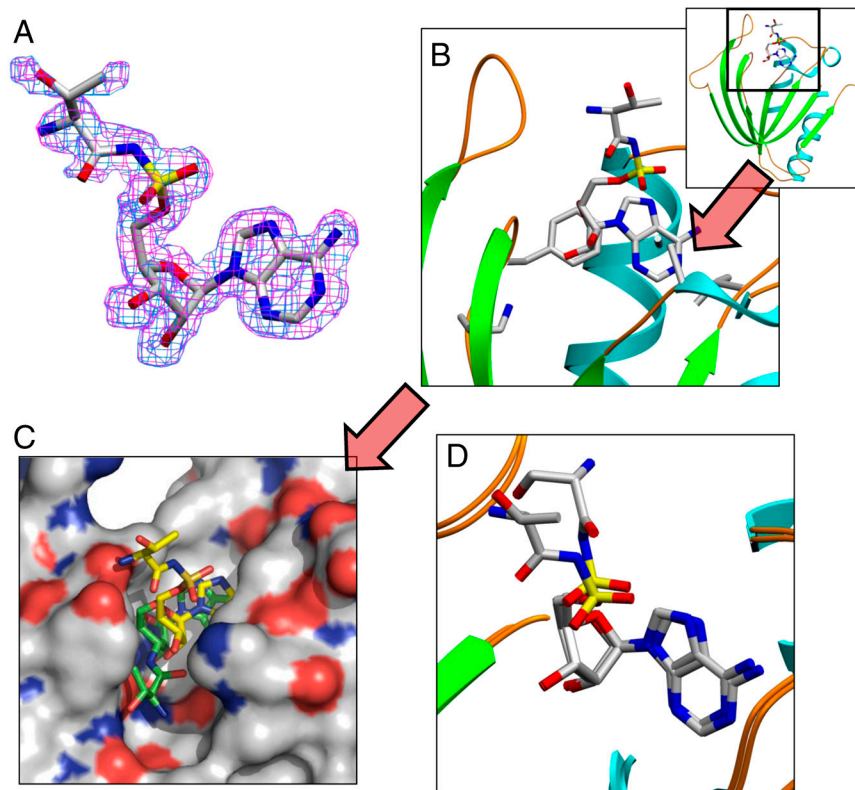


**Fig. 54.** Pab-NTD-ThrAMS complex - A glimpse of pretransfer cognate substrate analog captured at the editing pocket. (A): Unbiased electron density maps ( $F_o - F_c$  map at  $1.6\sigma$  in pink and  $2F_o - F_c$  map at  $0.8\sigma$  in blue) at 2.29 Å resolution for ThrAMS. (B): Enlarged view of ThrAMS protruding out of the editing pocket with no residues in its vicinity for enzymatic hydrolysis. The adenosine occupies the pocket defined by conserved residues in Pab-NTD as observed in other complexes. Inset: Overall view of the Pab-NTD-ThrAMS complex showing the threonyl moiety positioned out of the editing pocket. (C): Surface representation of editing pocket of Pab-NTD. ThrAMS (yellow) protrudes out of the editing pocket while Thr3AA (green) is positioned in the editing pocket. (D): Superposition of Pab-NTD-ThrAMS and Pab-NTD-SerAMS (PDB id: 2HL2) shows similar conformation of both pretransfer analogs. The adenosine moieties are observed in identical position in both complex whereas the aminoacyl moiety of ThrAMS is positioned out of the editing pocket in a similar conformation as that observed for SerAMS demonstrating a lack of cognate-noncognate discrimination that is hallmark of any editing activity.

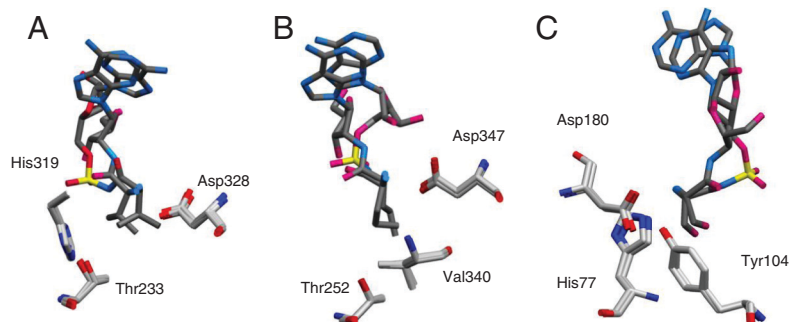


**Fig. 55.** Similar mode of cognate discrimination in other editing domains. (A): Superposition of post and pretransfer complexes in CP1 domain of IleRS. Val2AA (PDB id: 1WNZ), ValAMS (PDB id: 1VK8), and residues Asp328, His319, and Thr233 as observed in pre and posttransfer complexes are shown. His319 and Thr233 are important for discriminating Ile-tRNA<sup>Ile</sup> in the editing pocket. Asp328 anchors the  $\alpha$ -amino group of valyl moiety of analogs. Closer view of Val2AA and ValAMS shows major change in the position of the adenosine moiety and significant change in the valyl position. Difference of 0.73 Å, 1.21 Å, 1.46 Å, and 2.02 Å in the corresponding position of C $\alpha$ , C $\beta$ , C $\gamma$ 1, and C $\gamma$ 2 atoms of Val is observed. Ile has an extra methyl group (C-C distance: 1.54 Å) at C $\gamma$ 1 atom when compared to Val. The difference in C $\gamma$ 1 atoms of Val in the two complexes is 1.46 Å, suggesting that the editing pocket may have room for Ile also. (B): Superposition of post and pretransfer complexes in CP1 domain of LeuRS. Nva2AA, and NvaAMS as observed in PDB id: 1OBC and 1OBH respectively. Asp347, Val340, and Thr252 in the editing pocket are shown. Thr252 is important for discriminating Leu-tRNA<sup>Leu</sup> in the editing pocket. Asp347 anchors the  $\alpha$ -amino group of norvalyl moiety of analogs. Closer view of Nva2AA and NvaAMS shows a significant difference in the position of adenosine moieties. The superposition also shows a difference of 0.26 Å, 0.72 Å, 1.36 Å, and 0.64 Å in the corresponding positions of C $\alpha$ , C $\beta$ , C $\gamma$ , and C $\delta$  atoms of norvaline (Nva). It is important to note that Leu has an extra methyl group at C $\gamma$  when compared to Nva that shows a maximum deviation of 1.36 Å. Thus, it seems reasonable to assume that an extra methyl group (C-C distance: 1.54 Å) of Leu can be accommodated in the pocket. (C): Superposition of post and pretransfer complexes in editing domain of bacterial ThrRS. L-Ser3AA and L-SerAMS as observed in PDB id: 1TKY and 1TKG respectively. His77, Tyr104, and Asp180 are proposed to be important for discriminating Thr-tRNA<sup>Thr</sup> in the editing pocket. Closer view of Ser3AA and SerAMS as observed in PDB id: 1TKY and 1TKG respectively, show substantial change in the position of the adenosine moiety compared to subtle but significant change in the aminoacyl moiety, e.g., the C atoms are 0.6 Å apart, C $\beta$  atoms are 0.55 Å apart, and side chain  $\gamma$ O atoms are 0.78 Å apart; keeping the same anchoring points in the editing pocket. The arrangement shows a relaxed requirement for the positioning of aminoacyl moiety suggesting that an extra methyl group of threonyl moiety can be accommodated in the pocket as we know from our study that a subtle rotation of C-C $\alpha$  axis is sufficient to accommodate the extra methyl group preventing any steric hindrance in case of Pab-NTD.

**Table S1. Crystallographic data collection and refinement statistics**

	Pab-NTD-Ser3AA complex	Pab-NTD-Thr3AA complex	Pab-NTD-Gly3AA complex	Pab-NTD-ThrAMS complex
Data collection				
Space group	$P2_12_12_1$	$P2_12_12_1$	$P2_12_12_1$	$P2_12_12_1$
Cell dimensions:				
a (Å)	37.2	38.3	40.3	42.3
b (Å)	66.3	65.9	69.1	72.1
c (Å)	93.2	93.7	94.7	96.6
Resolution range (Å) *	25.0 – 1.86 (1.93 – 1.86)	25.0 – 1.86 (1.93 – 1.86)	25.0 – 2.40 (2.49 – 2.40)	25.0 – 2.29 (2.37 – 2.29)
Total observations	116,119 (9,892)	100,085 (7,540)	49,972 (3,590)	50,699 (3,297)
Unique reflections	20,015 (1,839)	20,386 (1,785)	10,812 (923)	13,334 (993)
Completeness (%)	99.5 (95.1)	98.5 (88.4)	98.7 (87.6)	95.9 (72.7)
Rmerge (%)	5.5 (15.1)	6.4 (29.1)	10.9 (29.1)	5.5 (20.2)
$\langle I/(\sigma) \rangle$	32.3 (9.1)	27.2 (3.9)	15.22 (3.5)	19.1 (3.4)
Redundancy	5.8 (5.4)	4.9 (4.3)	4.6 (3.9)	3.8 (3.0)
Data refinement				
Resolution (Å)	1.86	1.86	2.40	2.29
No. of reflections	19,966	20,336	10,776	13,296
R (%)	19.49	19.79	21.43	22.21
$R_{\text{free}}$ (%) <sup>†</sup>	22.05	22.89	27.44	29.03
Monomers / a.u.	2	2	2	2
No. of residues	290	288	289	289
No. of atoms	2,520	2,523	2,452	2,513
Protein	2,304	2,273	2,281	2,299
Ligand	50	52	46	60
Water	166	198	125	144
rms deviation				
Bond lengths (Å)	0.005	0.005	0.007	0.007
Bond angles (°)	1.36	1.40	1.48	1.50
Mean B value (Å <sup>2</sup> )	18.4	28.0	31.8	35.1
Protein	17.9	27.1	31.8	34.7
Ligand	13.8	23.2	26.0	48.3
Water	27.4	39.5	34.0	34.6

\*Values in parentheses are for the highest-resolution shell.

<sup>†</sup>Throughout the refinement, 5% of the total reflections were held aside for  $R_{\text{free}}$ .

**Table S2. Different ratio of Pab-NTD:Ligand used for cocrystallization to capture the ligands**

Ligands	Pab-NTD:ligand ratio	Electron density of ligand observed (Yes/No)
Ser3AA	1:25	Yes
	1:2	Yes
	1:1	No crystal obtained
Thr3AA	1:25	Yes
	1:4	Yes
	1:3	No crystallization attempts
	1:2	No
Gly3AA	1:1	No crystal obtained
	1:25	Yes
	1:2	Yes
ThrAMS	1:1	No crystal obtained
	1:25	Yes
	1:50	No
Free Thr	1:50	No
Ser2AA	1:50	No
Gly2AA	1:50	No

Protein concentration used in crystallization set up was 200  $\mu$ M.

**Table S3. Multiple Pab-NTD complexes for each ligand**

Ligands	Pab-NTD complexes
Ser3AA	13 independent observations in 7 different crystals at resolutions: 1.86 Å, 1.86 Å, 1.96 Å, 2.00 Å, 2.20 Å, 2.20 Å, and 2.25 Å.
Thr3AA	6 independent observations in 3 different crystals at resolutions: 1.86 Å, 2.20 Å, and 2.71 Å.
Gly3AA	4 independent observations in 2 crystals at resolutions: 2.40 Å and 1.86 Å*

All (but one Pab-NTD-Ser3AA complex in I222) complexes were obtained in same space group ( $P2_12_12_1$ ). \*Data completion for this particular Pab-NTD-Gly3AA complex was only 76.6% and hence not presented here. However, clear densities for Gly3AA, W1, and W2 were observed in unbiased electron density maps.

**Table S4. Refined B-factor values of W1, W2 and their neighboring atoms**

	Ser3AA (Monomer A)	Ser3AA (Monomer B)	Thr3AA (Monomer A)	Thr3AA (Monomer B)
W1 (catalytic water)	22.66	26.08	Absent	Absent
$\epsilon$ -amino group of Lys121	20.47	25.79	30.72	33.19
2' OH of analog	13.33	16.59	21.25	23.77
W2	14.83	14.17	23.68	18.85
$\alpha$ -amino group of analog	12.43	11.64	20.88	22.89
$\beta$ -hydroxyl of analog	14.34	14.25	23.46	23.73
Side chain OH of Tyr79	12.17	11.17	21.74	21.36
Carbonyl O of Lys121	12.32	11.78	19.13	21.47

**Table S5. Direct as well as water mediated interaction of Lys121 with Ser3AA and Thr3AA**

	Direct interaction: Lys121 Ccarbonyl and $\gamma$ -OH group of analog	W2 mediated interaction of Lys121 carbonyl and $\gamma$ -OH group of analog. Lys121(CO)- W2, W2- $\gamma$ -OH distances	Direct interaction of Lys121 $\alpha$ -amino group and $\gamma$ -OH group of analog.	W2 mediated interaction of Lys121 carbonyl and $\alpha$ -amino group of analog. Lys121(CO)-W2, W2- $\alpha$ - amino group distances	Direct interaction: Lys121e-NH <sub>2</sub> and 2' OH of analog	Direct interaction: Lys121e-NH <sub>2</sub> and C $\alpha$ analog (van der Waals)	W1 mediated interaction of Lys121e-NH <sub>2</sub> and 2' OH of analogLys121e-NH <sub>2</sub> -W1, W1-2' OH of analog
Thr3AA (monomer A)	3.67 Å	2.59 Å, 3.36 Å	3.20 Å	2.59 Å, 2.78 Å	3.39 Å	3.55 Å	Absent
Thr3AA (monomer B)	3.70 Å	2.66 Å, 3.32 Å	3.19 Å	2.66 Å, 2.70 Å	3.80 Å	3.73 Å	Absent
Ser3AA (monomer A)	3.55 Å	2.65 Å, 3.15 Å	3.04 Å	2.65 Å, 2.76 Å	(Absent)	4.04 Å	2.53 Å, 2.70 Å
Ser3AA (monomer B)	3.53 Å	2.76 Å, 3.17 Å	3.06 Å	2.76 Å, 2.65 Å	(Absent)	4.19 Å	2.44 Å, 2.65 Å